Polymeric Metal–Nucleotide Complexes. The Crystal Structures of [(C₉H₁₂N₃O₈P)Cd(H₂O).H₂O]ₙ and [(C₉H₁₂N₃O₈P)Co(H₂O)]ₙ Formed between Cadmium(II) or Cobalt(II) Ions and Cytidine 5'-Monophosphate

$$[(C_9H_{12}N_3O_8P)Cd(H_2O).H_2O]_n \text{ and } [(C_9H_{12}N_3O_8P)Co(H_2O)]_n$$

By George R. Clark* and John D. Orbell

Department of Chemistry, The University of Auckland, Auckland, New Zealand

The structures of the polymeric complexes formed between Cd^{II} or Co^{II} ions and the pyrimidine nucleotide cytidine 5'-monophosphate (CMP), $[(C_9H_{12}N_3O_8P)Cd(H_2O).H_2O]_n$ and $[(C_9H_{12}N_3O_8P)Co(H_2O)]_n$, have been determined by X-ray diffraction. Crystals of Cd–CMP are orthorhombic, $a = 5.294$ (1), $b = 17.070$ (1), $c = 16.371$ (1) Å, $Z = 4$, $\rho_c = 2.11$ g cm^{-3}, space group $P2_12_12_1$. $R = 0.038$ and $R_w = 0.045$ for 1104 reflections with $I > \sigma(I)$. The Cd atom is in a distorted square-pyramidal environment consisting of N(3) of the pyrimidine ring, three O atoms of different phosphate groups, and a water molecule. The complex is three-dimensionally polymeric, with cylindrical channels, consisting of cross-linked —Cd—O—P—O—Cd— spirals. The sugar ring is puckered C(3')-*endo*, and the conformation about the glycosidic C—N bond is *anti*. Crystals of Co–CMP are monoclinic, $a = 10.002$ (1), $b = 7.459$ (2), $c = 9.429$ (1) Å, $\beta = 96.58$ (1)°, $Z = 2$, $\rho_c = 1.89$ g cm^{-3}, space group $P2_1$. $R = 0.073$ and $R_w = 0.063$ for 871 reflections with $I > \sigma(I)$. The Co atom is tetrahedrally coordinated to N(3) of the cytosine ring, to a water molecule, and to two O atoms from two different phosphate groups, giving a two-dimensional layer structure. The sugar ring pucker is C(2')-*endo*/C(1')-*exo*, and the conformation about the glycosidic C—N bond is *anti*. The bases are stacked with an average separation of 3.73 Å.

Introduction

The influence of metal ions on the properties and reactivity of nucleic acids has been widely studied in recent years. Investigations of model systems have been concerned with the complexes formed between metal ions and nucleic acid constituents, *i.e.* the bases, sugars, nucleosides, and nucleotides, with crystal structure analyses establishing binding sites and conformational parameters for a diversity of such complexes (Hodgson, 1977).

Most nucleotide complexes whose structures have been determined are those incorporating purine bases. These complexes are generally either (i) monomeric, with bonding between the metal atom and N(7) of the purine base, and with all remaining coordination sites occupied by water molecules, or (ii) polymeric, still with the metal–N(7) bond, but with the metal atom coordinated directly to O atoms of phosphate groups. It is not clear what factors are responsible for the adoption of a particular geometry, but from a recent X-ray study it appears that the monomeric geometry is adopted when some metal ions complex with tRNA molecules (Jack, Ladner, Rhodes, Brown & Klug, 1977).

We have prepared single crystals of the Cd and Co complexes derived from the pyrimidine nucleotide cytidine 5'-monophosphate [Cd–CMP, Co–CMP], and

_____

* To whom correspondence should be addressed.

in a preliminary account have described their structures as being respectively three- and two-dimensionally polymeric (Clark & Orbell, 1975). We now present details of their refined structures. The crystal structure of a monoclinic polymorph of Cd–CMP has been reported (Bau, Gellert & Shiba, 1975).

Experimental

Small crystals of the two compounds were prepared by the method of Ogawa & Sakaguchi (1972). After preliminary X-ray photography, the crystals most suitable for intensity collection were positioned on a Hilger & Watts four-circle automated diffractometer but were deliberately mis-set from crystallographic axes to minimize the effects of multiple diffraction. Cell dimensions were derived by least squares from the diffractometer setting angles of twelve general reflections (Busing & Levy, 1967). Crystal data are given in Table 1.

Intensities were collected for $\theta \leq 56.5°$ with a symmetric $2\theta/\omega$ scan of 1.40° in 2θ at a scan rate of $0.01°$ s^{-1}. The background was recorded at each end of the scan range with stationary counts of 10s for Cd–CMP and 15s for Co–CMP. The diameters of the primary- and diffracted-beam collimators were 1.4 and 3.5 mm respectively. During data collection, the intensities of three standard reflections were remeasured periodically, but no non-statistical

Table 1. *Crystal data*

	Cd–CMP	Co–CMP
Empirical formula	$C_9H_{16}N_3O_{10}PCd$	$C_9H_{14}N_3O_9PCo$
M_r	469.7	398.1
a	5.294 (1) Å	10.002 (1) Å
b	17.070 (1)	7.459 (2)
c	16.371 (1)	9.429 (1)
β		96.58 (1)°
V	1479.4 Å³	698.8 Å³
T	290 ± 1 K	293 ± 1 K
λ(Cu $K\alpha$)	1.5418 Å	1.5418 Å
Z	4	2
$F(000)$	936	406
D_c	2.11 g cm⁻³	1.89 g cm⁻³
μ	136.1 cm⁻¹	108.0 cm⁻¹
Space group	$P2_12_12_1$	$P2_1$
Systematic extinctions	h odd for h00 k odd for 0k0 l odd for 00l	k odd for 0k0
Mosaic spread	0.09°	0.16°
Crystal size	0.16 × 0.080 × 0.04 mm (white needles)	0.14 × 0.06 × 0.03 mm (purple-blue needles)

variations were encountered. No reflection for either compound exceeded a count rate of 7000 s⁻¹ and thus attenuators were not required. The data sets were corrected for Lorentz and polarization effects. For Cd–CMP, 1104 unique reflections were recorded with $I > \sigma(I)$ $[\sigma(I) = \{T + [t/(t_1 + t_2)]^2 + (B_1 + B_2) + (pI)^2\}^{1/2}$, where T is total count in scan time t, B_1 and B_2 are background counts in times t_1 and t_2, and p was assigned an initial value of 0.04, but this was later increased to 0.07 on the basis of a weighting-scheme agreement analysis (Corfield, Doedens & Ibers, 1967)]. A further 78 reflections were deemed unobserved and were not used in the calculations. For Co–CMP, 871 unique reflections were obtained for which $I > \sigma(I)$. A further 135 were considered unobserved. The p factor used, 0.04, was found to be satisfactory. Absorption corrections were applied during the latter stages of refinement, the maximum and minimum transmission coefficients being 0.78 and 0.43 respectively for Cd–CMP, and 0.73 and 0.47 respectively for Co–CMP.

Structure determination and refinement

Atomic coordinates for the metal atoms were deduced from Patterson syntheses, while those for the remaining non-hydrogen atoms were obtained from subsequent electron density maps. Scattering factors were from *International Tables for X-ray Crystallography* (1962), values for Cd, Co, and P being adjusted for dispersion effects. Refinement of atomic parameters used the full least-squares matrices. The function minimized was $\sum w(|F_o| - |F_c|)^2$, weights, w, being $4F_o^2/\sigma^2(F^2)$.

Cd–CMP

Two refinement cycles with isotropic temperature factors, followed by one cycle in which the Cd and P atoms were assigned anisotropic thermal parameters, reduced R from 0.31 (for Cd only) to 0.071, and R_w to 0.079 $\{R_w = [\sum w(|F_o| - |F_c|)^2/\sum w|F_o|^2]^{1/2}\}$. Analysis of the weighting scheme revealed that the function $\langle \sum w(|F_o| - |F_c|)^2 \rangle$ was not constant over the full range of F_o values, and therefore the p term in the calculation of $\sigma(I)$ was increased from 0.04 to 0.07 to further downweight the more intense reflections. The next two cycles reduced R and R_w to 0.065 and 0.075 respectively and produced satisfactory weighting analyses. The absolute configuration of the crystals was then determined by repeating the last two cycles with inverted atomic coordinates. R and R_w were 0.085 and 0.100 respectively, and the chirality is deduced to be that consistent with the atomic coordinates in Table 2.

The absence of any large maxima in a difference synthesis verified the basic structure, but the resolution was such that not all the H atoms could be located. Accordingly, only the eight H atoms whose positions could be calculated on the basis of expected molecular

Table 2. *Atomic parameters for* Cd–CMP

Standard deviations are in parentheses. H atoms are in calculated positions.

	x	y	z
Cd	−0.1488 (2)	0.6632 (1)	0.4462 (1)
P	0.6123 (6)	0.2534 (2)	0.1262 (2)
O(2)	0.1841 (14)	0.5290 (4)	0.4720 (4)
O(3)	0.4944 (13)	0.1719 (4)	0.1351 (4)
O(4)	0.8924 (13)	0.2498 (4)	0.1121 (4)
O(5)	0.4704 (22)	0.3026 (6)	0.0656 (6)
O(1')	0.6863 (15)	0.3983 (4)	0.3478 (4)
O(2')	0.5198 (18)	0.3499 (4)	0.5234 (4)
O(3')	0.4529 (28)	0.2175 (7)	0.4287 (8)
O(5')	0.5828 (21)	0.2980 (6)	0.2131 (6)
O(W1)	−0.4431 (22)	0.6088 (6)	0.5416 (6)
O(W2)	0.8274 (17)	0.4791 (4)	0.5848 (4)
N(1)	0.3149 (17)	0.4713 (4)	0.3528 (5)
N(3)	−0.0188 (25)	0.5660 (7)	0.3561 (7)
N(4)	−0.2339 (31)	0.5982 (8)	0.2396 (8)
C(2)	0.1607 (23)	0.5241 (5)	0.3946 (6)
C(4)	−0.0530 (32)	0.5590 (8)	0.2737 (9)
C(5)	0.1058 (34)	0.5060 (9)	0.2309 (10)
C(6)	0.2875 (32)	0.4644 (9)	0.2700 (10)
C(1')	0.5021 (22)	0.4286 (6)	0.4013 (6)
C(2')	0.3892 (22)	0.3617 (6)	0.4480 (6)
C(3')	0.4370 (35)	0.2911 (9)	0.3917 (10)
C(4')	0.6943 (19)	0.3132 (6)	0.3539 (6)
C(5')	0.7680 (26)	0.2780 (7)	0.2738 (7)
H(C5)	0.1128	0.4909	0.1721
H(C6)	0.4006	0.4301	0.2372
H(C1')	0.5898	0.4658	0.4428
H(C2')	0.1993	0.3703	0.4552
H(C3')	0.3072	0.2880	0.3465
H(C4')	0.8338	0.2958	0.3910
H(C5')	0.9374	0.3002	0.2546
H(C5')'	0.7853	0.2198	0.2770

geometries were included. These atoms were assigned fixed isotropic temperature factors of $4 \cdot 0$ $Å^2$. Their positions were not refined. The data were then corrected for absorption before the final cycles were computed. Refinement converged with $R = 0 \cdot 038$ and $R_w = 0 \cdot 045$ and with a maximum shift/error of $0 \cdot 2$. Final atomic parameters are given in Table 2.

Table 3. *Atomic parameters for* Co–CMP

Standard deviations are in parentheses. H atoms are in calculated positions.

	x	y	z
Co	0·0672 (2)	0·2500	0·3399 (2)
P	0·1868 (4)	0·6111 (7)	−0·4888 (4)
O(2)	0·2791 (8)	0·2614 (19)	0·1971 (9)
O(3)	0·2412 (8)	0·7464 (19)	−0·5838 (9)
O(4)	0·0878 (9)	0·4865 (14)	−0·5668 (11)
O(5)	0·1246 (9)	0·6988 (11)	−0·3675 (10)
O(W)	0·1558 (10)	0·0660 (15)	0·4710 (11)
O(1′)	0·3736 (9)	0·4444 (16)	−0·1228 (11)
O(2′)	0·4222 (10)	−0·0256 (17)	−0·1604 (12)
O(3′)	0·6252 (9)	0·1902 (13)	−0·1956 (11)
O(5′)	0·3043 (9)	0·4841 (15)	−0·4250 (11)
N(1)	0·2133 (10)	0·2544 (23)	−0·0447 (12)
N(3)	0·0589 (9)	0·2425 (19)	0·1284 (10)
N(4)	−0·1708 (10)	0·2385 (22)	0·0609 (12)
C(2)	0·1901 (11)	0·2473 (26)	0·0961 (14)
C(4)	−0·0469 (13)	0·2473 (29)	0·0196 (15)
C(5)	−0·0189 (13)	0·2642 (28)	−0·1208 (14)
C(6)	0·1097 (12)	0·2618 (31)	−0·1496 (15)
C(1′)	0·3528 (12)	0·2680 (28)	−0·0785 (13)
C(2′)	0·3819 (14)	0·1496 (21)	−0·2016 (16)
C(3′)	0·4965 (12)	0·2544 (27)	−0·2648 (14)
C(4′)	0·4757 (13)	0·4459 (21)	−0·2186 (15)
C(5′)	0·4224 (15)	0·5681 (22)	−0·3454 (18)
H(C5)	−0·0790	0·2847	−0·2148
H(C6)	0·1289	0·2683	−0·2554
H(C1′)	0·4195	0·2384	0·0086
H(C2′)	0·2987	0·1382	−0·2741
H(C3′)	0·4847	0·2448	−0·3754
H(C4′)	0·4418	0·5233	−0·3074
H(C5′)	0·3995	0·6847	−0·3038
H(C5′)	0·4970	0·3834	−0·4063

Table 4. *Bond lengths* (Å) *for non-hydrogen atoms in* Cd–CMP

Standard deviations are in parentheses.

Cd–N(3)	2·324 (12)	C(1′)–C(2′)	1·499 (15)
Cd–O(W1)	2·394 (11)	C(2′)–C(3′)	1·538 (20)
Cd–O(3)	2·267 (7)	C(3′)–C(4′)	1·543 (20)
Cd–O(4)	2·222 (11)	C(4′)–O(1′)	1·457 (12)
Cd–O(5)	2·248 (7)	O(1′)–C(1′)	1·409 (13)
N(3)–C(4)	1·366 (19)	C(2′)–O(2′)	1·429 (13)
C(4)–N(4)	1·295 (21)	C(3′)–O(3′)	1·397 (21)
C(4)–C(5)	1·420 (22)	C(4′)–C(5′)	1·494 (16)
C(5)–C(6)	1·356 (23)	C(5′)–O(5′)	1·437 (17)
C(6)–N(1)	1·368 (18)	P–O(5′)	1·621 (11)
N(1)–C(2)	1·395 (13)	P–O(3)	1·532 (8)
C(2)–O(2)	1·276 (13)	P–O(4)	1·502 (11)
C(2)–N(3)	1·346 (16)	P–O(5)	1·501 (8)
N(1)–C(1′)	1·464 (13)		

Co–CMP

Refinement of atomic parameters for Co–CMP closely paralleled that for Cd–CMP. R was $0 \cdot 46$ for Co only and $0 \cdot 19$ after all non-hydrogen atoms had been located. Two cycles with isotropic temperature factors, followed by two for which the Co and P atoms were assigned anisotropic thermal parameters, reduced R and R_w to $0 \cdot 087$ and $0 \cdot 076$ respectively. Analysis of the weighting scheme showed that the value $0 \cdot 04$ for p in the calculation of $\sigma(I)$ was well chosen. The absolute configuration was again established by replacing x,y,z with $−x,−y,−z$ for all atoms. Refinement returned R and R_w as $0 \cdot 105$ and $0 \cdot 093$ respectively. Therefore the correct chirality corresponds to the original model (Table 3). A difference synthesis failed to locate all the H atoms, and only those whose positions could be predicted were included in subsequent calculations. The data were corrected for absorption before the final cycles. In view of the small number of observed reflections, no further atoms were assigned anisotropic thermal parameters. The final R and R_w were $0 \cdot 073$ and $0 \cdot 063$ respectively.

Interatomic distances and angles are listed in Tables 4 and 5 for Cd–CMP and in Tables 6 and 7 for Co–CMP.*

Computations

All calculations were performed on the University of Auckland Burroughs B6718 computer. Programs used were: *HILGOUT*, for data processing; *DABS*, a modification of *DATAPH*, described by Coppens (1969); *FOURIER* and *CUCLS* from the University of Canterbury, New Zealand; and *ORTEP* (Johnson, 1965).

Description of the structures

Cd–CMP

The Cd atom is pentacoordinated, to the cytosine base at N(3), a water molecule, and three O atoms (each from a different phosphate group). As a result, the crystals exist as three-dimensional polymers. Extending throughout the crystals are spiralling columns of the sequence −Cd−O−P−O−Cd−, the turns of which are cross-linked by additional Cd−phosphate bridges. The nucleotide units interconnect the columns, by spanning from the phosphate

---

Table 5. Bond angles (°) for non-hydrogen atoms in Cd–CMP

Standard deviations are in parentheses.

N(3)—Cd—O(W1)	109·3 (4)	N(1)—C(2)—O(2)	118·2 (9)	C(2')—C(3')—O(3')	117·0 (13)
N(3)—Cd—O(3)	85·0 (4)	N(3)—C(2)—O(2)	119·9 (10)	O(3')—C(3')—C(4')	109·9 (13)
N(3)—Cd—O(4)	91·2 (4)	C(2)—N(3)—Cd	106·9 (8)	C(3')—C(4')—C(5')	119·0 (13)
N(3)—Cd—O(5)	127·8 (4)	C(4)—N(3)—Cd	130·5 (10)	C(5')—C(4')—O(1')	110·4 (9)
O(W1)—Cd—O(3)	83·3 (3)	N(3)—C(4)—N(4)	118·6 (14)	C(4')—C(5')—O(5')	109·5 (10)
O(W1)—Cd—O(4)	159·4 (4)	C(5)—C(4)—N(4)	123·7 (15)	C(5')—O(5')—P	115·4 (9)
O(W1)—Cd—O(5)	78·9 (3)	C(6)—N(1)—C(1')	124·5 (10)	C(1')—C(2')—O(2')	110·8 (9)
O(3)—Cd—O(4)	101·4 (3)	C(2)—N(1)—C(1')	116·9 (8)	O(5')—P—O(3)	107·7 (5)
O(3)—Cd—O(5)	146·4 (2)	O(1')—C(1')—C(2')	108·3 (8)	O(5')—P—O(4)	104·4 (6)
O(4)—Cd—O(5)	86·8 (3)	C(1')—C(2')—C(3')	103·1 (10)	O(5')—P—O(5)	105·6 (5)
N(3)—C(4)—C(5)	117·7 (14)	C(2')—C(3')—C(4')	101·2 (11)	O(3)—P—O(4)	112·3 (5)
C(4)—C(5)—C(6)	121·4 (14)	C(3')—C(4')—O(1')	104·2 (9)	O(3)—P—O(5)	111·5 (4)
C(5)—C(6)—N(1)	119·9 (14)	C(4')—O(1')—C(1')	110·1 (8)	O(4)—P—O(5)	114·5 (5)
C(6)—N(1)—C(2)	118·7 (10)	N(1)—C(1')—O(1')	108·3 (8)	Cd—O(3)—P	109·4 (4)
N(1)—C(2)—N(3)	121·8 (10)	N(1)—C(1')·C(2')	112·7 (9)	Cd—O(4)—P	134·1 (6)
C(2)—N(3)—C(4)	120·6 (12)	O(2')—C(2')—C(3')	109·1 (10)	Cd—O(5)—P	120·6 (4)

Table 6. Bond lengths (Å) for non-hydrogen atoms in Co–CMP

Standard deviations are in parentheses.

Co—N(3)	1·987 (11)	C(1')—C(2')	1·512 (21)
Co—O(W)	1·988 (10)	C(2')—C(3')	1·560 (21)
Co—O(4)	1·972 (10)	C(3')—C(4')	1·514 (21)
Co—O(5)	2·001 (9)	C(4')—O(1')	1·437 (17)
N(3)—C(4)	1·389 (20)	O(1')—C(1')	1·397 (18)
C(4)—N(4)	1·342 (21)	C(2')—O(2')	1·409 (18)
C(4)—C(5)	1·389 (23)	C(3')—O(3')	1·454 (18)
C(5)—C(6)	1·344 (23)	C(4')—C(5')	1·550 (21)
C(6)—N(1)	1·351 (21)	C(5')—O(5')	1·467 (18)
N(1)—C(2)	1·376 (20)	P—O(5')	1·575 (11)
C(2)—O(2)	1·232 (18)	P—O(3)	1·492 (11)
C(2)—N(3)	1·380 (19)	P—O(4)	1·491 (11)
N(1)—C(1')	1·469 (20)	P—O(5)	1·511 (10)

of one column, through the sugar and base, to the Cd of an adjacent column. Fig. 1 is a perspective view of a segment of the crystal network and shows the atomic numbering scheme, the overall nucleotide geometry, and the anisotropic thermal ellipsoids (depicted as 50% probability boundaries). Fig. 2 is a stereodiagram

showing the column of cross-linked —Cd—O—P—O—Cd— spirals.

Cd is well known for its ability to exist in a variety of different coordination arangements, with between four and eight donor atoms. Often the Cd atom is in two, or even three, different chemical environments in the one crystal, and often the complexes are polymeric (Harrison & Trotter, 1972).
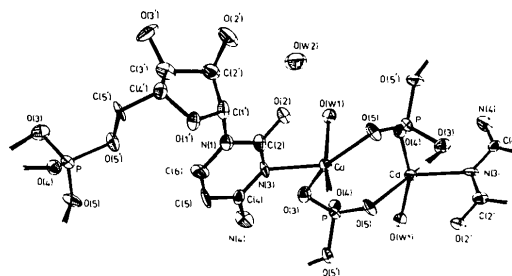

Fig. 1. Metal coordination and nucleotide geometry in Cd–CMP.

Table 7. Bond angles (°) for non-hydrogen atoms in Co–CMP

Standard deviations are in parentheses.

|					
N(3)—Co—O(W)	124·8 (4)	C(4)—N(3)—Co	133·1 (10)	C(2')—C(3')—O(3')	108·5 (11)
N(3)—Co—O(4)	117·6 (4)	N(3)—C(4)—N(4)	115·9 (14)	O(3')—C(3')—C(4')	109·1 (12)
N(3)—Co—O(5)	101·1 (4)	C(5)—C(4)—N(4)	124·9 (15)	C(3')—C(4')—C(5')	112·3 (12)
O(W)—Co—O(4)	108·9 (4)	C(6)—N(1)—C(1')	120·5 (13)	C(5')—C(4')—O(1')	106·5 (11)
O(W)—Co—O(5)	98·9 (4)	C(2)—N(1)—C(1')	118·6 (12)	C(4')—C(5')—O(5')	109·3 (12)
O(4)—Co—O(5)	99·6 (4)	O(1')—C(1')—C(2')	105·7 (12)	C(5')—O(5')—P	117·5 (9)
N(3)—C(4)—C(5)	119·2 (14)	C(1')—C(2')—C(3')	102·3 (12)	O(5')—P—O(3)	109·2 (6)
C(4)—C(5)—C(6)	119·4 (15)	C(2')—C(3')—C(4')	103·4 (12)	O(5')—P—O(4)	103·9 (6)
C(5)—C(6)—N(1)	121·7 (15)	C(3')—C(4')—O(1')	107·4 (11)	O(5')—P—O(5)	108·9 (6)
C(6)—N(1)—C(2)	120·7 (13)	C(4')—O(1')—C(1')	109·8 (11)	O(3)—P—O(4)	113·1 (6)
N(1)—C(2)—N(3)	118·7 (13)	N(1)—C(1')—O(1')	107·8 (12)	O(3)—P—O(5)	111·7 (6)
C(2)—N(3)—C(4)	120·1 (12)	N(1)—C(1')—C(2')	108·4 (10)	O(4)—P—O(5)	109·7 (6)
N(1)—C(2)—O(2)	123·8 (14)	C(1')—C(2')—O(2')	113·8 (12)	Co—O(4)—P	143·9 (6)
N(3)—C(2)—O(2)	117·1 (13)	O(2')—C(2')—C(3')	111·7 (12)	Co—O(5)—P	131·5 (6)
C(2)—N(3)—Co	106·6 (9)				
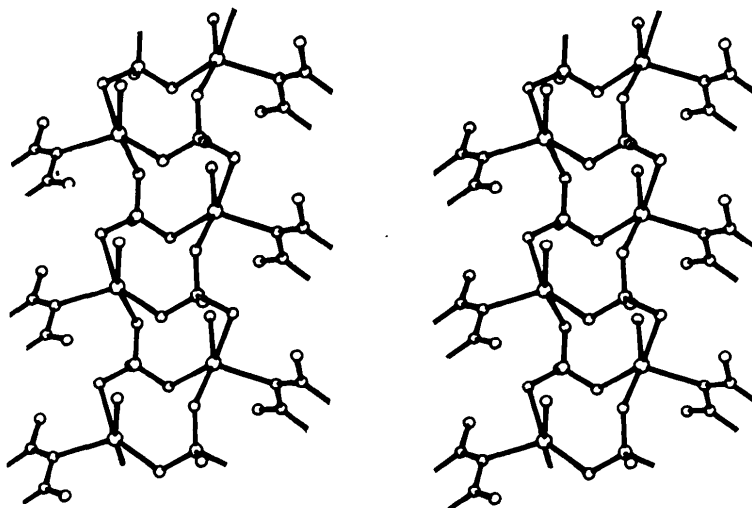
Fig. 2. Stereopair showing the interlinked Cd polyhedra in Cd—CMP.

The stereochemistry in Cd–CMP is that of a distorted square pyramid. The apex is occupied by N(3) of the cytosine ring with Cd—N(3) 2·324 (12) Å. The three phosphate O donors are approximately equidistant at 2·222 (11), 2·248 (7) and 2·267 (7) Å, but the water molecule is further away at 2·397 (11) Å. These distances lie within the range of values observed in other compounds. When the coordination number is higher than five the Cd—O bonds are often longer. The square-pyramidal array of donor atoms is severely distorted from its ideal geometry. All bond angles for Cd–CMP are listed in Table 5 and the deviations from 180° of the angles between the trans-planar bonds (146·4 and 159·4°) indicate the extent of the distortion. Also, the angle N(3)—Cd—O(5), ideally 90°, is 127·8°. These distortions are similar to those found in many Cd complexes (Harrison & Trotter, 1972; Post & Trotter, 1974; Maslen, Greaney, Ralston & White, 1975).

The coordination geometry in the present compound can be compared with that of its monoclinic polymorph (Bau, Gellert & Shiba, 1975). There the Cd is seven-coordinated with bonds to N(3) (2·35 Å), to four O atoms of phosphate groups (ave. 2·37 Å), to a water

molecule (2·32 Å), and also to O(2) of the cytosine ring (2·69 Å). Cd—O(2) is longer than the others but still lies within the range observed in other complexes, especially those of high coodination number. From the geometry it appears to be a true bond. The corresponding distance between Cd and O(2) in the present (orthorhombic) form is 2·92 Å but now no bond is envisaged. That the two polymorphs adopt different coordination geometries whilst forming intricate, but different, polymeric networks, is a further manifestation of the remarkable facility with which Cd assumes particular stereochemistries to conform to the forces being experienced on crystallization.
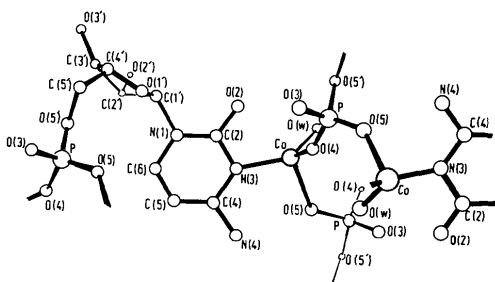

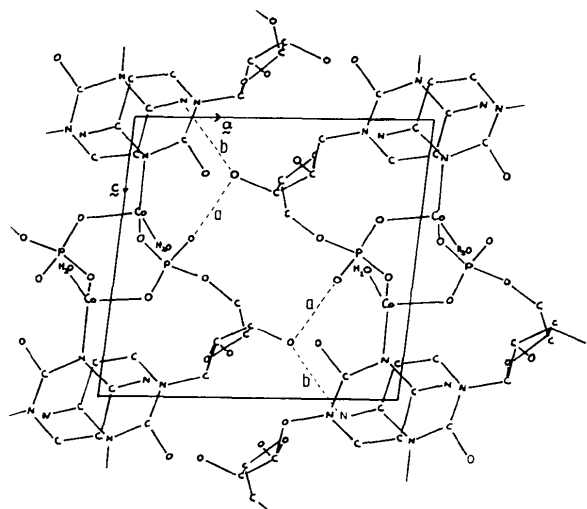Fig. 3. Metal coordination and nucleotide geometry in Co–CMP.

Fig. 4. The layer structure of Co–CMP as seen in the (010) projection.

Co–CMP

The Co atom lies within a distorted tetrahedral arrangement consisting of N(3) of the cytosine base [Co–N(3), 1·987 (11) Å], a water molecule [Co–O(W), 1·988 (10) Å], and two O atoms (each from a different phosphate group) [Co–O(4), 1·972 (10); Co–O(5), 2·001 (9) Å]. The distortion of the tetrahedron is such that the angles at Co range from 98·9 (4) to 124·8 (4)°, but, even so, these angles are not outside the range commonly found. The overall stereochemistry and nucleotide geometry are shown in Fig. 3, with the atomic numbering scheme.

Because of the manner in which the Co bonds to O atoms of different phosphate groups, the crystals exist as two-dimensional polymers. Fig. 4 shows the undulations of the layer structure. The directions of propagation of the layers are along **b** and **c**, and successive layers are only held together by two unique hydrogen bonds. In the figure, the stacking of the cytosine bases perpendicular to **b** is seen.

Cytosine ring geometries

The six atoms of the cytosine rings are planar in both Cd–CMP and Co–CMP, but the exocyclic atoms are significantly displaced from the planes. Details are given in Tables 8 and 9. Pyrimidine geometries have been well documented (Voet & Rich, 1970). The bond lengths and angles in the present compounds compare with those observed in a variety of other compounds containing cytosine (Barker & Marsh, 1964; Jeffrey & Kinoshita, 1963; McClure & Craven, 1973), protonated cytosine (Trus & Marsh, 1972; Kindberg & Amma, 1975), and cytidine (Furberg, Petersen & Rømming, 1965; Szalda, Marzilli & Kistenmacher, 1975). Unfortunately, the rather large standard deviations render inconclusive any detailed comparisons.

Trus & Marsh (1972) have observed a pronounced readjustment of the cytosine ring angles consequent upon protonation. In particular, there is a bond widening at N(3), the site of protonation, by approximately 6°, from 120 to 126°. They observed this for two independent molecules of 1-methylcytosine hydrochloride, and it is also found in $(CytH^+)_2PdCl_4$ (Kindberg & Amma, 1975). The corresponding angles in Cd–CMP and Co–CMP are 120·6 (12) and 120·1 (12)° respectively, and thus metal coordination has not altered the ring geometries.

Geometries of the β-ribofuranose rings

The geometries of the sugar rings in Cd–CMP and Co–CMP are described by the bond lengths and angles of Tables 4, 5, 6 and 7; by the least-squares-plane calculations of Tables 8 and 9, and by the torsion angles of Table 10.

The ribofuranose rings of nucleosides and nucleotides are puckered, usually into one of two preferred conformations, described as C(3')-*endo* and C(2')-*endo* (Sundaralingam, 1969). Either C(3') or C(2') is displaced, by between 0·4 and 0·6 Å, from the plane of the other four atoms of the ring, in a direction towards C(5'). An atom displaced in the opposite sense is termed *exo*. Tables 8 and 9 show that in Cd–CMP the sugar pucker is C(3')-*endo*, but that in Co–CMP it is in a less common conformation, C(2')-*endo*/C(1')-*exo*. A more precise description of the ribofuranose conformation is given by the torsion angles about each bond. Various authors have adopted different conventions for assigning symbols to selected angles, for reference to polynucleotide backbone sequences, and these are indicated in the table. To aid comparison with other

Table 8. *Least-squares planes for* Cd–CMP

The equations of the planes are given in direction-cosine form with reference to the cell axes. Asterisks denote atoms defining the planes. Displacements of the atoms from the planes are given in Å.

(a) The cytosine ring

$$0.663X + 0.733Y - 0.153Z - 6.125 = 0$$

C(4)*	−0.004	N(1)*	−0.007	N(4)	−0.064
C(5)*	−0.002	C(2)*	0.008	O(2)	−0.042
C(6)*	0.018	N(3)*	−0.002	C(1')	−0.004

(b) The ribose ring

$$-0.703X - 0.081Y - 0.706Z - 7.120 = 0$$

C(1')*	0.017	C(4')*	0.009	O(3')	0.175
C(2')*	−0.010	O(1')*	−0.009	O(5')	0.710
C(3')	0.561	O(2')	−1.352	C(3')-*endo*	

The angle between planes (a) and (b) is 114·7°.

Table 9. *Least-squares planes for* Co–CMP

The equations of the planes are given in direction-cosine form with reference to orthogonalized axes. Asterisks denote atoms defining the planes. Displacements of the atoms from the planes are given in Å.

(a) The cytosine ring

$$0.002X - 0.998Y - 0.058Z - 1.875 = 0$$

C(4')*	0.023	N(1)*	0.009	N(4)	0.061
C(5')*	−0.026	C(2)*	−0.016	O(2)	−0.174
C(6')*	0.010	N(3)*	0.000	C(1')	−0.071

(b) The ribose ring

(i) $$-0.694X - 0.007Y - 0.720Z + 1.926 = 0$$

O(1')*	0.048	C(2')	0.480	C(4')*	−0.085
C(1')*	0.010	C(3')*	0.059	C(2')-*endo*	

(ii) $$-0.580X + 0.201Y - 0.790Z - 0.650 = 0$$

O(1')*	−0.016	C(2')*	0.029	C(4')*	0.045
C(1')	−0.460	C(3')*	−0.049	C(1')-*exo*	

The angles between plane (a) and planes (bi) and (bii) are 87·3 and 98·9° respectively.

Table 10. *Torsion angles involving ribose rings*

Conventions adopted by (a) Sundaralingam (1969), (b) Altona & Sundaralingam (1972) and (c) Seeman, Rosenberg, Suddath, Kim & Rich (1976).

	a	b	c	Cd–CMP	Co–CMP
C(6)–N(1)–C(1')–O(1')	χ	χ	χ	16·1°	69·7°
C(6)–N(1)–C(1')–C(2')				−76·4	−46·9
C(4')–O(1')–C(1')–C(2')	τ_0	θ_3		−2·5	−30·7
O(1')–C(1')–C(2')–C(3')	τ_1	θ_4		−24·1	33·8
C(1')–C(2')–C(3')–C(4')	τ_2	θ_0		34·6	−24·4
C(2')–C(3')–C(4')–O(1')	τ_3	θ_1		−33·5	7·5
C(3')–C(4')–O(1')–C(1')	τ_4	θ_2		20·1	14·2
C(4')–O(1')–C(1')–N(1)				−120·0	−152·2
N(1)–C(1')–C(2')–C(3')				84·3	−151·6
N(1)–C(1')–C(2')–O(2')				−147·7	−87·7
O(1')–C(1')–C(2')–O(2')				87·5	154·5
O(2')–C(2')–C(3')–O(3')				36·2	−30·8
O(2')–C(2')–C(3')–C(4')				−83·2	−146·5
C(1')–C(2')–C(3')–O(3')				154·0	91·3
C(2')–C(3')–C(4')–C(5')				−157·0	−109·3
O(3')–C(3')–C(4')–C(5')	ψ'		ζ	78·7	135·4
O(3')–C(3')–C(4')–O(1')				−157·9	−107·8
C(5')–C(4')–O(1')–C(1')				148·9	134·8
O(1')–C(4')–C(5')–O(5')				−61·6	−66·3
C(3')–C(4')–C(5')–O(5')	ψ		ε	58·7	51·2
C(4')–C(5')–O(5')–P	φ		δ	−171·0	143·5
C(5')–O(5')–P–O(3)	ω		γ	99·0	56·6
C(5')–O(5')–P–O(4)				−38·5	−177·5
C(5')–O(5')–P–O(5)				−160·7	−65·7

compounds containing ribose rings, Altona & Sundaralingam (1972) advocate a pseudorotation model in which the value of the phase angle of pseudorotation, P, is representative of the nature of the ribose pucker. The amplitude of pucker is characterized by the parameter τ_m. Generally, the ribose rings fall into two narrow sectors on the pseudorotation cycle with values of P lying in the ranges 0 to 18° [C(3')-*endo*] and 144 to 180° [C(2')-*endo*]. For Cd–CMP and Co–CMP the observed values of P are 16·72 and 136·53° respectively. These values correspond to C(3')-*endo* and C(2')-*endo*/C(1')-*exo*. The amplitudes of pucker, τ_m, are 36·13 for Cd–CMP and 33·62 for Co–CMP. The actual atomic displacements from the best planes of the other ring atoms are: for Cd–CMP, C(3') displaced by 0·56 Å from the best plane through O(1'), C(1'), C(2') and C(4'); for Co–CMP, C(2') displaced by 0·48 Å from the best plane through O(1'), C(1'), C(3') and C(4'), or, alternatively, C(1') displaced by −0·46 Å from the best plane through O(1'), C(2'), C(3') and C(4'). These displacements are of normal magnitude.

In both complexes the conformation about C(4')–C(5') is *gauche–gauche* (Shefter & Trueblood, 1965).

Orientation of the bases

The relative orientation between ribose and base is given by the glycosyl torsion angle χ_{CN} (Sundaralingam & Jensen, 1965). The observed angles are

Table 11. *Hydrogen-bonding interactions in* Cd–CMP

(a) Symmetry position of atom (2): (1) x,y,z; (2) $\frac{1}{2} - x, -y, \frac{1}{2} + z$; (3) $\frac{1}{2} + x, \frac{1}{2} - y, -z$; (4) $-x, \frac{1}{2} + y, \frac{1}{2} - z$. (b) Unit-cell translations of atom (2).

Atom (1)···Atom (2)		(a)	(b)		
O(W2)···O(2)	2·78 Å	1	1	0	0
O(W2)···O(2')	2·92	1	0	0	0
O(W2)···O(W1)	2·73	1	1	0	0
N(4)···O(W2)	2·90	2	0	1	−1
O(W1)···O(2)	2·66	1	−1	0	0
N(4)···O(3)	2·77	4	0	0	0
O(3')···O(2')	2·68	3	−1	0	1

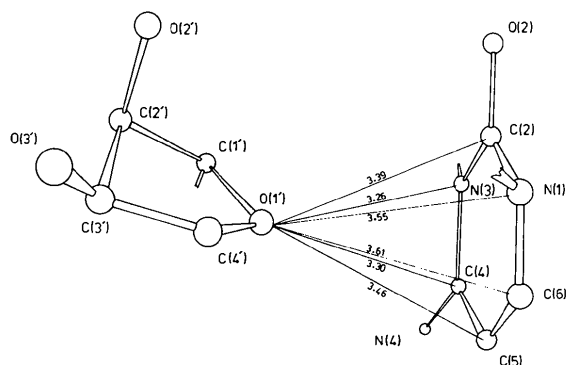|			
O(W1)···O(W2)···O(2')	103·3°	Cd–O(W1)···O(2)	113·8°
O(W1)···O(W2)···O(2)	86·3	Cd–O(W1)···O(W2)	98·2
O(W1)···O(W2)···N(4)	120·4	C(2)–O(2)···O(W1)	122·1
O(2')···O(W2)···O(2)	112·5	C(2)–O(2)···O(W2)	125·1
O(2')···O(W2)···N(4)	82·1	C(4)–N(4)···O(3)	106·5
O(2)···O(W2)···N(4)	146·9	C(4)–N(4)···O(W2)	105·5

Fig. 5. View of the stacking interaction between O(1') and the cytosine ring in Cd–CMP.

16·1 and 69·7° for Cd–CMP and Co–CMP respectively, and thus both are in the *anti* domain, as has been found in all nucleotide structures.

Hydrogen-bonding interactions

Cd–CMP. Proposed hydrogen bonds for Cd–CMP are listed in Table 11. The network structure is clearly influenced by the four hydrogen bonds about the uncoordinated water molecule O(W2). Table 11 also lists the angles of these bonds about O(W2) which give an approximately tetrahedral array. O(2') is involved in hydrogen bonds but not O(3') (the reverse of Co–CMP). O(2) and N(4) are each involved in two hydrogen bonds.

Co–CMP. There appear to be only two intermolecular hydrogen-bonding interactions present in Co–CMP. Each corrugated double layer has a tightly-knit central Co/phosphate spiral which, with the stacking of the bases, keeps the layers compact. The double layers are seen in Fig. 4. Only O(3') projects towards a neighbouring layer and forms hydrogen bonds: O(3')···O(3) 2·62 and O(3')···N(4) 3·01 Å.

The angle O(3)···O(3')···N(4) is 105·0°. These interactions serve to hold the layers together. In the diagram the apparent close contact between O(3') and O(2) does not represent a hydrogen bond, as the O(3')···O(2) distance is 3·34 Å. The only intralayer contact which may represent a hydrogen bond is N(4)···O(5) 2·89 Å.

Base-stacking interactions

Two types of base-stacking interactions are frequently observed in nucleic acid constituents and in polynucleotides. The more common type involves the partial overlap of nearly parallel bases of neighbouring molecules. The purine and pyrimidine heterocyclic rings possess considerable charge asymmetry, and the stacking forces appear to result from the electrostatic interaction between the hetero-atoms of one base and a polarizable π-electron system of the other. There is considerable interest in this type of stacking, as it serves as a model for the anti-cancer behaviour of those aromatic compounds which are believed to intercalate between the stacked bases of the nucleic acids.

The second stacking interaction is less well known. It involves the stacking between O(1') of a ribose ring and a neighbouring purine or pyrimidine base, such that O(1') is approximately equidistant from all the atoms of the base ring. These two types of base-stacking interactions have been reviewed by Bugg, Thomas, Sundaralingam & Rao (1971) and further described for the crystal structures of UpA (Sussman, Seeman, Kim & Berman, 1972), ApU (Seeman, Rosenberg, Suddath, Kim & Rich, 1976) and GpC (Rosenberg, Seeman, Day & Rich, 1976).

In the present study it is found that O(1')–base stacking occurs in Cd–CMP, whereas in Co–CMP there is base–base stacking. In Cd–CMP, O(1') is symmetrically positioned with respect to a neighbouring cytosine ring. This geometry is depicted in Fig. 5 together with the distance of O(1') from each member of the ring. These distances are somewhat greater than those found in most other examples (Sussman, Seeman, Kim & Berman, 1972); nevertheless it is likely that this stacking interaction plays a significant role in determining the overall polymeric geometry. Possibly similar weak stacking interactions exist in other crystals without having been remarked upon, since secondary crystal-packing forces are generally not well understood. Rosenberg, Seeman, Day & Rich (1976) note differences in ribose conformations which appear to correlate with the presence or absence of stacking involving O(1') but any assessment is not yet quantitative. The sugar ring conformation in Cd–CMP is C(3')-endo while that in Co–CMP [where there is base–base rather than O(1')–base stacking] is C(2')-endo/C(1')-exo. In Co–CMP the average stacking separation distance of the approximately planar pyrimidine rings is 3·73 Å and the stacking is

promulgated from one unit cell to the next by the b-axis repeat. The stacking can be seen in Fig. 4. The degree or extent of overlap is approximately one third of the normal (Bugg, Thomas, Sundaralingam & Rao, 1971).

References

ALTONA, C. & SUNDARALINGAM, M. (1972). J. Am. Chem. Soc. 94, 8205–8212.
BARKER, D. L. & MARSH, R. E. (1964). Acta Cryst. 17, 1581–1587.
BAU, R., GELLERT, R. W. & SHIBA, J. K. (1975). Abstracts. 7th International Conference on Organometallic Chemistry, Venice, Italy, September 1–5, p. 238.
BUGG, C. E., THOMAS, J. M., SUNDARALINGAM, M. & RAO, S. T. (1971). Biopolymers, 10, 175–219.
BUSING, W. R. & LEVY, H. A. (1967). Acta Cryst. 22, 457–464.
CLARK, G. R. & ORBELL, J. D. (1975). J. Chem. Soc. Chem. Commun. pp. 697–699.
COPPENS, P. (1969). International Summer School on Crystallographic Computing, Ottawa. Paper G1.
CORFIELD, P. W. R., DOEDENS, R. J. & IBERS, J. A. (1967). Inorg. Chem. 6, 197–204.
FURBERG, S., PETERSEN, C. S. & RØMMING, C. (1965). Acta Cryst. 18, 313–320.
HARRISON, W. & TROTTER, J. (1972). J. Chem. Soc. Dalton Trans. pp. 956–960.
HODGSON, D. J. (1977). Prog. Inorg. Chem. 23, 211–254.
International Tables for X-ray Crystallography (1962). Vol. III, pp. 202–206, 214–215. Birmingham: Kynoch Press.
JACK, A., LADNER, J. E., RHODES, D., BROWN, R. S. & KLUG, A. (1977). J. Mol. Biol. 111, 315–328.
JEFFREY, G. A. & KINOSHITA, Y. (1963). Acta Cryst. 16, 20–28.
JOHNSON, C. K. (1965). ORTEP. Report ORNL-3794. Oak Ridge National Laboratory, Tennessee.
KINDBERG, B. L. & AMMA, E. L. (1975). Acta Cryst. B31, 1492–1494.
McCLURE, R. J. & CRAVEN, B. M. (1973). Acta Cryst. B29, 1234–1238.
MASLEN, E. N., GREANEY, T. M., RALSTON, C. L. & WHITE, A. H. (1975). J. Chem. Soc. Dalton Trans. pp. 400–402.
OGAWA, M. & SAKAGUCHI, T. (1972). Yakugaku Zasshi, 92, 1166–1169.
POST, M. L. & TROTTER, J. (1974). J. Chem. Soc. Dalton Trans. pp. 674–678.
ROSENBERG, J. M., SEEMAN, N. C., DAY, R. O. & RICH, A. (1976). J. Mol. Biol. 104, 145–167.
SEEMAN, N. C., ROSENBERG, J. M., SUDDATH, F. L., KIM, J. J. P. & RICH, A. (1976). J. Mol. Biol. 104, 109–144.
SHEFTER, E. & TRUEBLOOD, K. N. (1965). Acta Cryst. 18, 1067–1077.
SUNDARALINGAM, M. (1969). Biopolymers, 7, 821–860.
SUNDARALINGAM, M. & JENSEN, L. H. (1965). J. Mol. Biol. 13, 914–929.
SUSSMAN, J. L., SEEMAN, N. C., KIM, S. H. & BERMAN, H. (1972). J. Mol. Biol. 66, 403–421.
SZALDA, D. J., MARZILLI, L. G. & KISTENMACHER, T. J. (1975). Biochem. Biophys. Res. Commun. 63, 601–605.
TRUS, B. L. & MARSH, R. E. (1972). Acta Cryst. B28, 1834–1840.
VOET, D. & RICH, A. (1970). Prog. Nucleic Acid Res. Mol. Biol. 10, 183–265.